

## Deep reactive ion etching of silicon moulds for the fabrication of diamond x-ray focusing lenses

This content has been downloaded from IOPscience. Please scroll down to see the full text.

2013 J. Micromech. Microeng. 23 125018

(<http://iopscience.iop.org/0960-1317/23/12/125018>)

View [the table of contents for this issue](#), or go to the [journal homepage](#) for more

Download details:

IP Address: 137.222.10.57

This content was downloaded on 12/11/2013 at 21:23

Please note that [terms and conditions apply](#).

# Deep reactive ion etching of silicon moulds for the fabrication of diamond x-ray focusing lenses

A M Malik<sup>1,2</sup>, O J L Fox<sup>3,4</sup>, L Alianelli<sup>3</sup>, A M Korsunsky<sup>2</sup>, R Stevens<sup>1,5</sup>,  
I M Loader<sup>1</sup>, M C Wilson<sup>1</sup>, I Pape<sup>3</sup>, K J S Sawhney<sup>3</sup> and P W May<sup>4</sup>

<sup>1</sup> Micro and Nanotechnology Centre, Science and Technology Facilities Council, Didcot, OX11 0QX, UK

<sup>2</sup> Department of Engineering Science, University of Oxford, Oxford, OX1 3PJ, UK

<sup>3</sup> Diamond Light Source Ltd, Didcot, OX11 0DE, UK

<sup>4</sup> School of Chemistry, University of Bristol, Bristol, BS8 1TS, UK

<sup>5</sup> School of Science and Technology, Nottingham Trent University, NG11 8NS, UK

E-mail: [lucia.alianelli@diamond.ac.uk](mailto:lucia.alianelli@diamond.ac.uk)

Received 31 July 2013, in final form 7 October 2013

Published 11 November 2013

Online at [stacks.iop.org/JMM/23/125018](http://stacks.iop.org/JMM/23/125018)

## Abstract

Diamond is a highly desirable material for use in x-ray optics and instrumentation. However, due to its extreme hardness and resistance to chemical attack, diamond is difficult to form into a structure suitable for x-ray lenses. Refractive lenses are capable of delivering x-ray beams with nanoscale resolution. A moulding technique for the fabrication of diamond lenses is reported. High-quality silicon moulds were made using photolithography and deep reactive ion etching. The study of the etch process conducted to achieve silicon moulds with vertical sidewalls and minimal surface roughness is discussed. Issues experienced when attempting to deposit diamond into a high-aspect-ratio mould by chemical vapour deposition are highlighted. Two generations of lenses have been successfully fabricated using this transfer-moulding approach with significant improvement in the quality and performance of the optics observed in the second iteration. Testing of the diamond x-ray optics on the Diamond Light Source Ltd synchrotron B16 beamline has yielded a line focus of sub-micrometre width.

(Some figures may appear in colour only in the online journal)

## 1. Introduction

### *1.1. Synchrotron optics fabricated from chemical vapour deposition (CVD) diamond*

Significant advances of x-ray techniques and the availability of new optics provide synchrotron users with beams of unprecedented brilliance and spatial resolution. Rapid progress in the development of optics has permitted a decrease in the size of focused x-ray beams, down to sub- $\mu\text{m}$  during the 1990s [1]. It is now considered realistic, although ambitious, to deliver x-ray beams of single digit nanometre size, with a measurable flux [2]. Imaging of materials on a nanometre scale will have an increasing impact on much fundamental and applied research. Construction of low-emittance synchrotron radiation sources, engineering efforts associated with high-

stability beams and end stations, and the design and fabrication of near-ideal x-ray optics are the contributing factors towards small, more-intense beams. Currently, synchrotron optics have extremely small focal lengths, down to a few mm, in order to demagnify the synchrotron sources to nanometre size. Refractive lenses offer one method by which x-ray beams can be nanofocused onto a sample, and advanced silicon microfabrication can be used to produce such optics with the desired aspect ratios and surface finish. Whilst single-crystal silicon possesses the high-quality material properties needed for high-aspect-ratio fabrication of nanofocusing lenses, its inherent absorption at x-ray wavelengths is not suited to high-flux applications, as refractive lenses are transmission devices and the x-ray path-length within a lens increases with decreasing the focal length. Diamond displays a multitude of exemplary properties making it desirable for x-ray optics

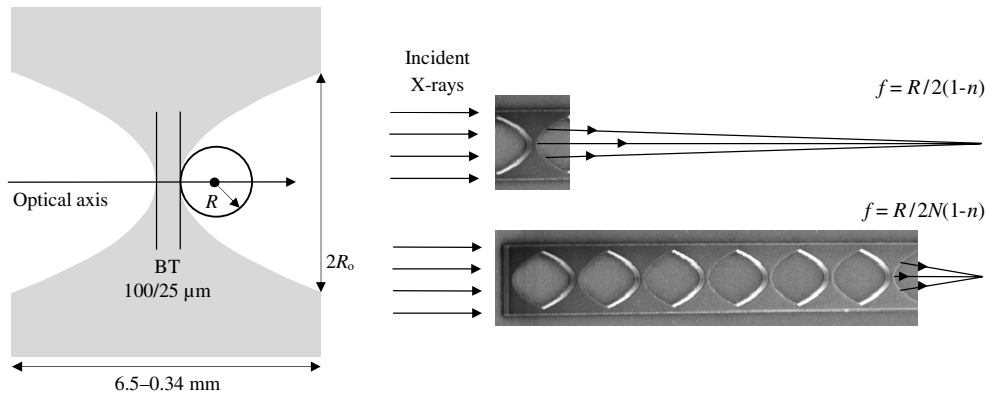


**Figure 1.** Schematic diagram of a single diamond refractive x-ray lens with parabolic profile, depicting the radius of curvature  $R$ , geometrical aperture  $2R_0$  and bridge thickness (BT). The BT is defined as the minimal distance between two lenses. SEM micrographs of a single diamond refractive lens and a diamond CRL consisting of a series of lenses that reduces the focal length.

and instrumentation, notably for high-brilliance third- and fourth-generation x-ray sources, where some materials cease to operate or remain stable due to the high intensity of the radiation pulses [3]. Its advantageous properties include: low atomic number, resulting in less photoelectric absorption than silicon optics as absorption scales as  $\sim Z^3$ ; relatively large decrement of the refractive index, so that less material is required to produce a short focal-length optic; high thermal conductivity; low thermal coefficient of expansion [4–6]. Nevertheless, processing diamond is technically challenging due to its chemical inertness and physical hardness. Several methods exist for patterning diamond, including laser micro-machining [7], ion-beam milling [8], dry etching [9–12] and selected-area deposition [13, 14]. We have developed a mould-based technique which has so far permitted fabrication of diamond lenses that concentrate the x-ray radiation onto a linear focus with a full-width at half-maximum (FWHM) of 400 nm. This is a novel fabrication method for synchrotron optics as it relies on both advanced silicon etch and diamond-controlled deposition techniques. The method can be used to fabricate very short focal diamond lenses for synchrotron applications.

### 1.2. Previous approaches to x-ray lens fabrication

Two general refractive optic designs are used for focusing synchrotron radiation. Compound refractive lenses (CRLs) consist of arrays of curved surfaces where each lens element further focuses the incident beam to achieve a short focal length [15]. The alternative design is a kinoform lens, in which the path length of radiation within the lens material is reduced; therefore, absorption and scattering of the beam are lower. In this paper, we report the fabrication of planar diamond CRLs with a typical design shown in figure 1. X-ray focusing lenses are fabricated with concave refractive surfaces as the refractive index of x-ray radiation in most materials is smaller than the refractive index in air. The focal length for paraxial rays,  $f$ , of the CRL shown in figure 1 is given by

$$f = \frac{R}{[(1-n)2N]} \quad (1)$$

Here,  $R$  is the surface curvature at the apex,  $n$  is the refractive index and  $N$  is the number of biconcave lenses in the array. It is challenging to make nanofocusing lenses with large acceptance, due to the absorption within the material reducing the effective aperture and to the limited aspect-ratio associated with the microfabrication methods. In practice, nanofocusing x-ray lenses often have apertures and depths no larger than  $100 \mu\text{m}$ .

The lenses fabricated using planar technologies focus in just one dimension. Two lenses can be used in crossed geometry to obtain a point focus of the x-ray source. X-ray planar lenses are currently used in synchrotron facilities to achieve beam sizes of 50 nm for nanoprobe experiments [16]. Our aim is to develop a lens with large aperture, low absorption and short (to very short) focusing distances  $f = 200$  to 20 mm. Zone plate optics with excellent imaging properties exist and with focal lengths in the required range. However, their efficiency is low at x-ray energies above 10 keV and, therefore, the need exists to develop an x-ray focusing lens with short focal length and high transmission.

X-ray beams delivered by synchrotron beamlines are high-resolution probes, capable of observing matter at the nanoscale due to their high spectral purity and collimation. The typical angular divergence of an undulator hard x-ray source at the Diamond Light Source synchrotron is  $10-20 \mu\text{rad}$ . Correct geometrical design of the lens shape is fundamental to avoid aberrations [17] and any deviation from the ideal shape will cause changes in the lens focal length and widening of the focused spot profile. A one-dimensional x-ray lens with non-vertical walls will also cause aberrations, as the profile of the lens changes with height, and its apex shifts according to the etch angle. A sidewall etch angle  $\alpha$  will cause a shift of the lens apex equal to  $\delta = t \times \tan(90^\circ - \alpha)$ . For a lens with thickness  $t = 50 \mu\text{m}$  and  $\alpha = 89.6^\circ$  (see section 3),  $\delta = 0.349 \mu\text{m}$ . The depth of field of the lenses described in this paper is  $d = 0.64 \times \lambda / (\text{NA})^2 \sim 250 \mu\text{m}$ , with  $\lambda$  being the radiation wavelength and NA the lens numerical aperture. The depth of field  $d$  is larger than the shift  $\delta$ ; therefore, the sidewall etch angle value is acceptable. However, a non-vertical etch also increases the effective radius  $R$  of the surfaces. The relative change in the focal length is proportional to the change in  $R$

and amounts to  $\Delta f/f \sim 0.6\%$  for the lenses described here (assuming that  $\Delta R = t \times \tan(90^\circ - \alpha)$ ), which is larger than the depth of field value. Surface roughness causes scattering of the x-ray radiation as quantified in [18] and any scalloping of the etched surface is a source of unwanted refraction orthogonal to the focusing plane.

Dry etching of chemical vapour deposition (CVD) diamond, using an oxygen plasma and a Cr mask, has been used to fabricate kinoform refractive lenses [5]. An etch depth of  $40 \mu\text{m}$  was achieved although the active part of the lens contributing to focusing was  $\sim 15 \mu\text{m}$  deep, because of the non-vertical sidewalls and surface roughness. Despite these issues, a focal width FWHM of  $3.2 \mu\text{m}$  was achieved at  $E = 17.5 \text{ keV}$ . Similarly, use of a cyclic, multi-step etch recipe, consisting of  $\text{O}_2$  with varying amounts of Ar, enabled a similar etch depth to be produced, but with a reduction in surface roughness. Synchrotron testing of these lenses resulted in a FWHM of  $1.0 \mu\text{m}$  at  $E = 11.3 \text{ keV}$  [6].

### 1.3. Diamond refractive optics using silicon mould microfabrication

Nanofocusing x-ray lenses require high-aspect-ratio sidewalls that are vertical and smooth [5, 6, 19] to minimize aberrations and parasitic scattering, respectively. A major drawback of the above-mentioned diamond micro-machining methods is that they can produce rough sidewalls, and in some cases this is coupled with a slow diamond etch rate. Recently reported dry etch rates of CVD diamond are in the range of  $3\text{--}11 \mu\text{m h}^{-1}$  [9–12]. The etch rate using ion-beam milling is even lower, for example, rates of  $0.72\text{--}1.2 \mu\text{m h}^{-1}$  have been reported [8]. To overcome these problems, an alternative method has been developed using a transfer-moulding technique [20, 21]. High-quality silicon moulds were made using well-established microelectronic techniques such as photolithography and deep reactive ion etching (DRIE) [22]. Nanocrystalline diamond (NCD) was deposited into these moulds using microwave plasma chemical vapour deposition (MWCVD). Finally, the diamond-containing moulds were bonded to handling substrates and the silicon mould was removed [4, 23]. The advantage of using this method is that the surface smoothness and sidewall verticality of the diamond lens is determined by that of the mould wall with high fidelity.

The Si DRIE step was carried out in an inductively coupled plasma etcher from Surface Technology Systems (STS), using the Bosch process [24]. The Bosch process is a cyclic etch and deposition process and depends upon a fine balance between its two components, namely, etching and passivation to produce high-aspect-ratio structures with vertical sidewalls. Furthermore, by adjusting the etch parameters, a range of profiles (positive/negative) can be produced [25]. A negative sidewall profile is defined here as a profile that becomes progressively narrower with increasing etch depth. Conversely, a positive profile becomes wider with etch depth, as shown in figure 2. A limitation of the Bosch process is that the sidewalls are rough with an undulating or scalloped surface produced due to the cyclic nature of the etch. Scalloping has a vertical and horizontal component, as shown in figure 3.

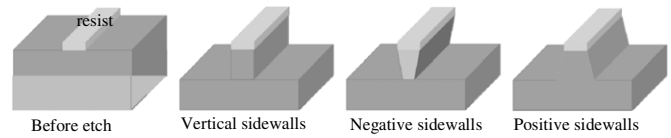


Figure 2. Different types of etched profiles.

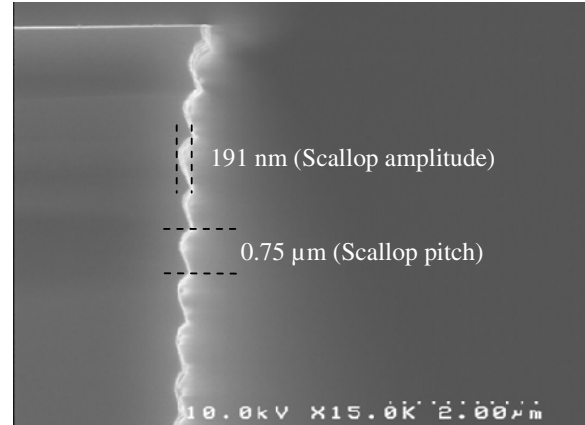


Figure 3. SEM cross-sectional micrograph showing scalloping produced by the Bosch process.

The use of polycrystalline diamond with as small a crystal size as possible, while maintaining the unique thermal and optical properties of single-crystal diamond, was important for fabricating optical components with minimal scattering and led to the choice of nanocrystalline material. Diamond material with a crystallite size between 30 and 50 nm still displays excellent thermal properties due to the close proximity of the diamond grains and with a thermal conductivity not significantly lower than bulk diamond. The amount of grain boundary material (non- $\text{sp}^3$ -bonded carbon) was kept to a minimum by using a plasma condition where  $\text{sp}^2$ -bonded surface groups are preferentially etched back into the gas phase.

The first generation of NCD CRLs produced by this method were tested on the B16 beamline [26] at the Diamond Light Source Ltd synchrotron and achieved beam focal widths of  $1.6 \mu\text{m}$  at  $E = 12 \text{ keV}$  (at a focal length of  $f = 0.56 \text{ m}$ ) and  $2.2 \mu\text{m}$  at  $E = 18 \text{ keV}$  (at  $f = 1.06 \text{ m}$ ) [23]. The CRL optics had a geometrical aperture of  $A = 300 \mu\text{m}$  although the deposition thickness limited the lens depth to  $D = 40 \mu\text{m}$ . Following improvements to the etch process, discussed in this paper, and optimization of the diamond deposition, a second generation of CRL samples was prepared. Synchrotron beamline tests of these nanofocusing optics are detailed below.

## 2. Experimental details

### 2.1. Si mould fabrication

The starting material for mould fabrication was 100 mm diameter,  $500 \pm 25 \mu\text{m}$  thick single-crystal Si wafers. The x-ray lens design, consisting of nine  $20 \times 20 \text{ mm}$  lens chips, was patterned with optical lithography. A  $2 \mu\text{m}$  layer of SU8-2 photoresist was spun onto a Si wafer followed by a soft bake

for 2 min at 95 °C on a hotplate. The resist was exposed to broadband UV radiation (MA6, SUSS MicroTec Lithography, GmbH) for 3 s with a power density of 10 mW cm<sup>-2</sup>. This was followed by a 60 s post-exposure bake at 95 °C. The wafers were then developed for 60 s at room temperature in a glass tank with EC solvent (Rohm and Haas Electronic Materials). Thereafter, the wafers were rinsed in isopropyl alcohol for 3 min. The surface area of the wafer to be etched was 5.7%, while the remainder was covered with the resist mask. After DRIE, the wafer was diced (Alpha, Oxford Lasers, UK) into its nine lens chips and the resist removed using Nano-strip™ heated to 75 °C. The etch depth, sidewall angle and scalloping were determined using SEM imaging (Hitachi S4000).

## 2.2. Diamond deposition and backside Si etch

NCD was deposited onto the 20 × 20 mm Si moulds using a 2.45 GHz MWCVD reactor, consisting of a vertically aligned cylinder where microwave (MW) power (typically  $P = 1$  kW) is fed into the sub-atmospheric cavity (typically  $p = 110$  Torr) through a quartz window [27]. Prior to deposition, the Si moulds were nucleated using an electrostatic spray of nanodiamond particles [28]. Deposition times for filling the mould were between 12 and 18 h using a CH<sub>4</sub>/N<sub>2</sub>/H<sub>2</sub> plasma gas mixture and a substrate temperature of  $T_{\text{sub}} \sim 1000$  K to achieve the desired NCD morphology. Tuning of the diamond grain size was achieved by adjusting the fraction of N<sub>2</sub> in the gas mixture. Using 0.7% N<sub>2</sub> in the total gas flow produced NCD with a grain size of 30–50 nm. The roughness of the refracting diamond surface was determined by the quality of the mould because the CVD-grown material fills the mould with sub-nanometre precision.

After diamond deposition, each sample was bonded to a 30 mm diameter handling substrate using epoxy glue (EPO-TEK® 353ND) and cured in an oven at 120 °C for 2 h. The handling substrates were thermal grade CVD diamond discs purchased from Element Six Ltd. The motivation for choosing CVD diamond was to minimize any stresses caused by thermal mismatch during the bonding thermal-cycle and when the lens is exposed to high-energy radiation. Subsequently, the STS etcher was used to etch the Si moulds from the chips and expose the diamond lenses (figure 4). Any residual stress caused by the lattice mismatch between the diamond film and the Si substrate is eliminated as the mould is etched away.

## 3. Results and discussion

### 3.1. Mould sidewall angle optimization

The control of the sidewall angle was achieved by changing the etch-to-passivation time ratio ( $R_{e/p}$ ) [29]. To determine the sensitivity of the lens design etch to the  $R_{e/p}$ , it was varied from 1.0 to 2.3, while keeping all other etch parameters constant. As the  $R_{e/p}$  was reduced from 2.3 to 1.0, the sidewall angle changed from  $\alpha = 88^\circ$  to  $\alpha = 91^\circ$ , i.e. the sidewall profile changed from a negative to a positive profile, figures 5 and 6(a). This was due to the passivation time being increased relative to the etch time. At an  $R_{e/p}$  of 1.5, a sidewall angle  $\alpha = 89.6^\circ$  was obtained with a clean etch floor. At an  $R_{e/p}$  of  $\leq 1.2$ , spikes of unetched

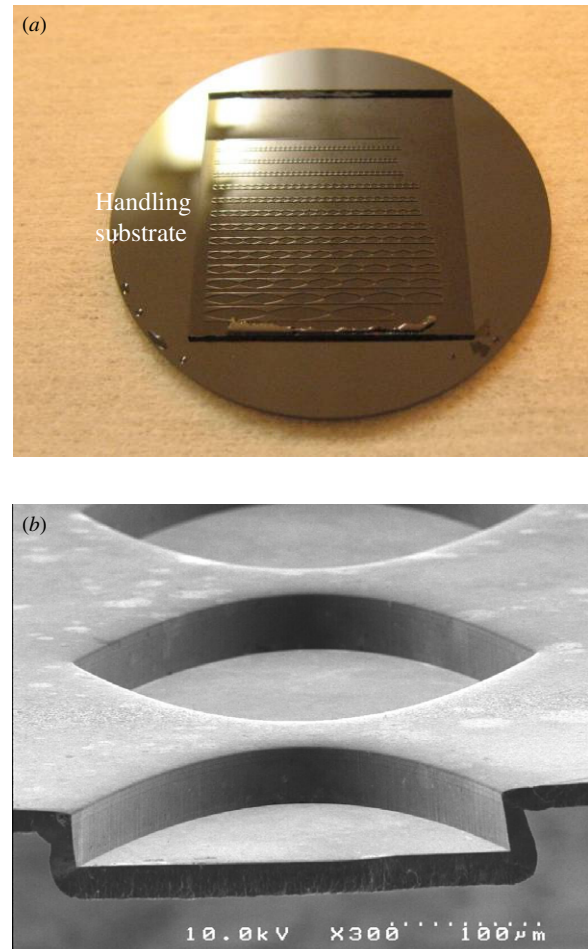


**Figure 4.** (a) Optical picture of diamond lenses after bonding and backside Si etch. (b) SEM micrograph of diamond lens, the smoothness of the sidewalls should be noted. The handling substrate is not present in image (b).

Si (known as ‘grass’ in etch terminology) were observed at the bottom of the etched trenches (figure 5). The origin of this is thought to be contamination on the wafer surface, as at this  $R_{e/p}$  value a positive profile is obtained and, therefore, any contamination will act like a micro-mask and grass formation will be observed.

At an  $R_{e/p}$  of 1.0, no etching took place because of the passivation stage being too dominant, and the etching becoming unbalanced. Another effect of decreasing the  $R_{e/p}$  was the reduction in the scallop amplitude and scallop pitch, figure 6(b). This can be explained by the fact that at a lower  $R_{e/p}$  there is a thicker passivation layer protecting the mould sidewalls and base, so it takes longer for the ions in the plasma to remove it before Si etching can begin. From these experiments, it can be concluded that an  $R_{e/p}$  of 1.5 produced the most vertical sidewall ( $\alpha = 89.6^\circ$ ) and no grass formation.

It should be noted that the bridge thickness (minimal distance between two lenses) was initially set to 100  $\mu\text{m}$ , see figure 1. However, the bridge thickness was reduced to 25  $\mu\text{m}$  for the next generation of lenses and the etch experiments conducted at a different  $R_{e/p}$  repeated. It was discovered that the sidewall angle was made more vertical by reducing the

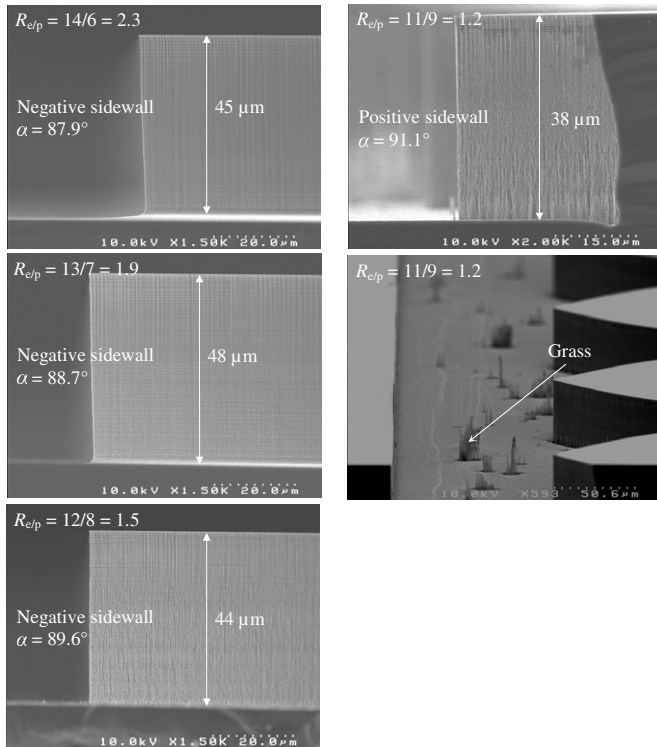


**Figure 5.** SEM micrographs showing how sidewall profile of the silicon lens mould changes for various  $R_{e/p}$ . As  $R_{e/p}$  is initially reduced, the sidewall profile becomes more vertical and the etched floor remains clean. However, as  $R_{e/p}$  is reduced to below 1.5, the sidewall profile changes from negative to positive and detrimental grass is observed on the etch floor.

bridge thickness. Thus, in addition to the dependence on  $R_{e/p}$ , the sidewall angle is affected by the bridge thickness.

### 3.2. Scalping minimization

In the previous section, it was shown that scalping was reduced by controlling the  $R_{e/p}$ . In an attempt to further reduce scalping, the effect of reducing the cycle time (the sum of one etch and one passivation step) of the Bosch process was investigated. By reducing the cycle time, the time spent etching the silicon per cycle is reduced; therefore, scalping is reduced. The cycle time was varied in the range of 12–20 s while maintaining an  $R_{e/p}$  of  $\sim 1.5$ . As the cycle time was reduced from 20 to 12 s, the scallop pitch was reduced from 0.58 to 0.47  $\mu\text{m}$ , while the scallop amplitude was reduced from 137 to 81 nm (figure 7). However, it was observed that the majority of the etched surfaces were subject to grass formation. Furthermore, at a cycle time of 12 s, no etching was observed. For a cycle time of 17 s, it was observed that the sidewall angle was near-vertical ( $\alpha = 89.7^\circ$ ); in fact, the best profile angle was obtained, albeit with some grass formation. Secondly, it was observed that the scalping was considerably less than that obtained with a cycle time of 20 s, and similar at cycle times  $< 17$  s (figure 7). It was anticipated that increasing the etch platen power would eliminate the grass formation and only marginally affect the profile angle. Thus, another etch experiment was conducted with the cycle time of 17 s and etch platen power of 16 W. A negative sidewall angle of  $\alpha =$

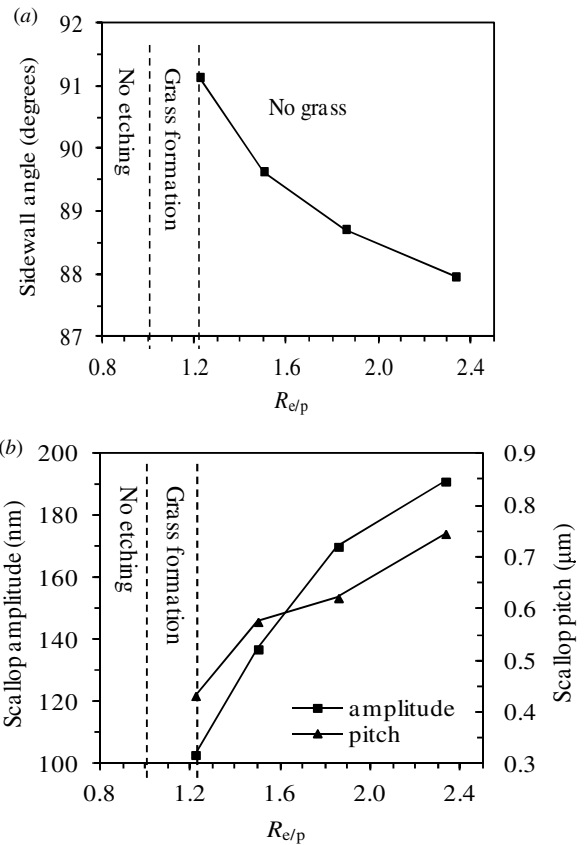


**Figure 6.** (a) Sidewall angle and (b) scalping as a function of  $R_{e/p}$ .

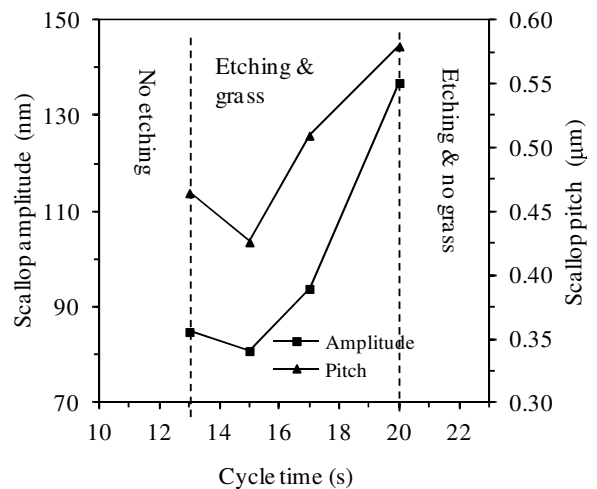


**Figure 7.** Scallop amplitude and pitch as a function of etch cycle time.

$89.4^\circ$  was obtained with scallop pitch of 0.53  $\mu\text{m}$  and scallop amplitude of 110 nm, and no grass formation. It should be noted that increasing etch platen power can adversely affect the profile angle. Therefore, it was increased in the cycle time that gave the near-vertical profile angle.

Hardware constraints limit the shortest cycle time possible on the Si etcher used in this investigation. However, there are deep Si etching instruments available which are capable of producing scalping amplitudes of less than 50 nm while maintaining clean etch floors and high Si etch rates by using fast gas-switching techniques [30].

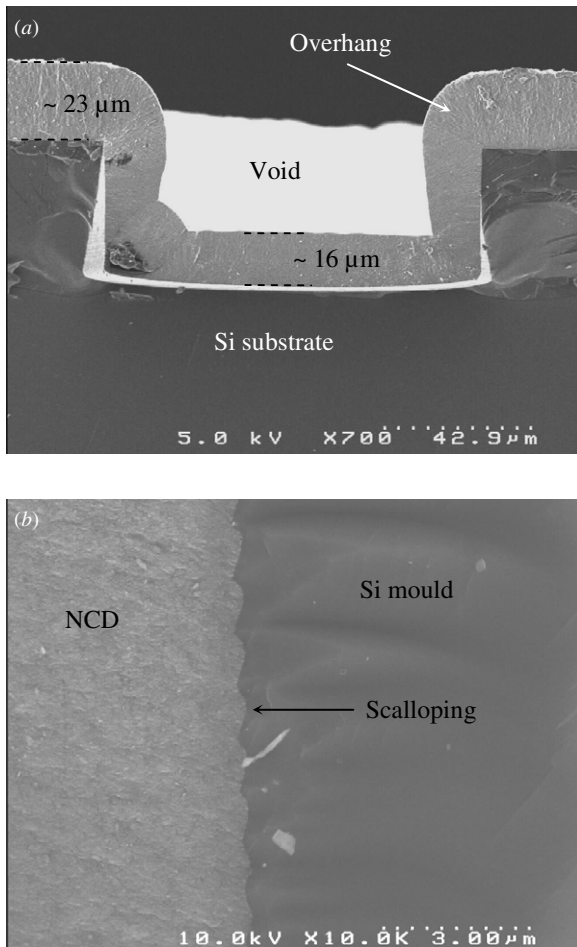


**Figure 8.** SEM micrographs of cleaved Si mould showing (a) incomplete NCD filling in lens region, overhang formation on mould edges and thicker NCD deposition on unetched region of mould, and (b) diamond CVD exhibiting excellent form fidelity.

### 3.3. Nanocrystalline diamond deposition

After initial NCD deposition trials, the samples were cleaved and examined using SEM to assess the success of the mould filling. It was observed that the diamond layer had not completely filled the etched regions, figure 8(a). For a working refractive lens, this region should be filled uniformly with diamond to at least the etch depth, so there is no parasitic refraction or light scattering from internal surfaces or voids. This issue is also apparent in the variation in the thickness of the NCD layer between the unetched (high) and etched (low) regions of the moulds and the formation of an overhang on the edges of the mould. It was observed that the NCD layer was thicker on the top, unetched surfaces of the mould than on the lower, etched regions. This difference in film thickness and the anisotropy in the mould filling it causes is due to both a variation in the surface temperature and the abundance of diamond-growth species ( $\text{CH}_3$  radicals) [27] which leads to a variable diamond deposition rate across the mould. The unetched areas have a higher surface temperature due to their proximity to the plasma and they experience a higher flux of active carbon-containing growth species. The overhang at the edge of the mould is a common feature of many deposition

processes, including sputtering, CVD and evaporation, and is formed because the deposition rate on the edge is higher than that on the sidewalls. The presence of the overhanging region of diamond is a concern as it can prevent further filling within the etched regions of the mould.

Although these test depositions highlighted a number of issues that would need to be addressed in subsequent work, the form fidelity of diamond in the silicon mould was remarkably good. The scalloping produced by the Bosch process is accurately replicated in the diamond layer, figure 8(b), and confirms the importance of reducing scalloping formed during the Si etch.

Adjustment of the MWCVD parameters during the deposition allowed an improved filling of the moulds so that suitable trial lens substrates could be fabricated, although complete filling was not possible. This was possible by carefully controlling the plasma, by changing the input power and chamber pressure, to maximize the diamond growth rate in the etched regions of the mould relative to the deposition rate on the top, unetched surfaces of the mould. Subsequent removal of the Si mould from these samples produced x-ray focusing optics, which could be tested on a synchrotron beamline.

### 3.4. X-ray test results and analysis

Over the course of optimizing both the mould etch process and the NCD deposition, two generations of suitable test lenses have been fabricated. Following improvements in the silicon mould etch and in the diamond nucleation and deposition processes, a second iteration of NCD nanofocusing optics was tested on the B16 test beamline [26] using a monochromatic beam of controlled spatial dimensions at a distance of  $P = 47$  m from the bending-magnet source. The planar CRL was mounted on a vertical focusing geometry and produced a well-defined focal spot. The spot shape and size were obtained by scanning a thin gold wire across the focal plane using a piezoelectric system and observing the change in intensity using a photodiode detector. The raw data and its derivative, which provides the focal spot width measurement, are shown in figure 9. A focal spot width FWHM of 400 nm was achieved at  $f = 0.19$  m and  $E = 11$  keV. While the calculated theoretical focus size of 275 nm was not achieved, due to additional broadening from lens aberrations, experimental variance and small-angle scattering, this experimental result, corresponding to a  $\times 247$  source demagnification, is remarkable and novel for a diamond x-ray lens.

The transfer moulding technique described here has produced lenses with smoother sidewalls than those obtained with dry etching [5, 6]. It should be noted that the moulded diamond lenses have a sidewall roughness commensurate with scalloping produced by the STS Si etcher. However, the scalloping can be reduced further by utilizing an advanced etcher or carrying out additional, post-etch processing like thermal oxidation [31]. The lenses developed here only have low aspect ratio, although future optics will require higher aspect ratios. Deposition of diamond into high-aspect-ratio moulds is not a trivial task and future research will focus on improving the diamond filling and minimizing overhang

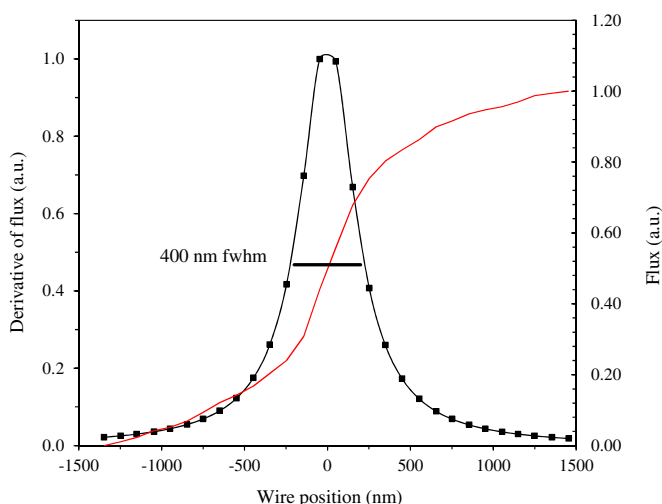


**Figure 9.** Focused spot measurement obtained by the knife edge method and fit of its derivative i.e. focused beam profile with FWHM of 400 nm.

formation. Scattering from the diamond grain boundaries is also a concern and a small angle x-ray scattering study is underway to determine its effect on lens performance.

#### 4. Conclusions

A silicon moulding process has been demonstrated to be a viable method to fabricate refractive NCD, nanofocusing x-ray lenses with vertical and smooth sidewalls. It was found that by optimizing the etch-to-passivation time ratio and etch cycle time of the Bosch process, Si moulds with vertical sidewalls and reduced scalloping could be fabricated. Examination of cleaved moulds after diamond CVD of the initial tests revealed incomplete diamond filling and the presence of an overhang on the mould edges, although the high form fidelity was remarkable. In the next set of diamond lenses, improved diamond filling and minimized overhang were achieved by altering the CVD process and the diamond nucleation. These diamond lenses proved to be capable of focusing the synchrotron radiation to sub- $\mu\text{m}$  size beams. Focal length reduction, and avoidance of excessive scattering by adopting a kinoform lens design, will allow further reduction of the focal spot size, towards a diffraction limited size. Small-angle x-ray scattering will be reduced through control of the mould etching and the MWCVD process. Improved filling of high-aspect-ratio Si moulds will allow production of lenses with wider apertures.

#### Acknowledgments

STFC are acknowledged for providing funding for diamond lens development through grant nos ST/F001665/1 and ST/F001606/1. OJLF was funded by EPSRC grant no EP/D074924/1. Diamond Light Source Ltd are acknowledged for providing beamtime on B16. AMK wishes to acknowledge

the support of EPSRC through grants EP/I020691 and EP/H003215.

#### References

- [1] Dhez P, Chevallier P, Lucatorto T B and Tarrío C 1999 *Rev. Sci. Instrum.* **70** 1907–20
- [2] Ice G E, Budai J D and Pang J W L 2011 *Science* **334** 1234–9
- [3] David C et al 2011 *Sci. Rep.* **1** 57
- [4] Snigirev A et al 2002 *Proc. SPIE* **4783** 1
- [5] Nohammer B, Hoszowska J, Freund A K and David C 2003 *J. Synchrotron Radiat.* **10** 168–71
- [6] Isakovic A F, Stein A, Warren J B, Narayanan S, Sprung M, Sandy A R and Evans-Lutterodt K 2009 *J. Synchrotron Radiat.* **16** 8–13
- [7] Park J K, Ayres V M, Asmussen J and Mukherjee K 2000 *Diam. Relat. Mater.* **9** 1154–8
- [8] Leech P W, Reeves G K, Holland A S and Shanks F 2002 *Diam. Relat. Mater.* **11** 833–6
- [9] Lee C L, Gu E, Dawson M D, Friel I and Scarsbrook G A 2008 *Diam. Relat. Mater.* **17** 1292–6
- [10] Silva F, Sussmann R S, Bénédic F and Gicquel A 2003 *Diam. Relat. Mater.* **12** 369–73
- [11] Tran D T, Fansler C, Grotjohn T A, Reinhard D K and Asmussen J 2010 *Diam. Relat. Mater.* **19** 778–82
- [12] Shiomi H 1997 *Japan. J. Appl. Phys.* **36** 7745–8
- [13] Shimada Y and Machi Y 1994 *Diam. Relat. Mater.* **3** 403–7
- [14] Masood A, Aslam M, Tamor M A and Potter T J 1991 *J. Electrochem. Soc.* **138** L67
- [15] Snigirev A, Kohn V, Snigireva I and Lengeler B 1996 *Nature* **384** 49–51
- [16] Schroer C G et al 2005 *Appl. Phys. Lett.* **87** 124103
- [17] Sanchez del R M and Alianelli L 2012 *J. Synchrotron Radiat.* **19** 366–74
- [18] Lengeler B, Schroer C G, Benner B, Günzler T F, Kuhlmann M, Tümmler J, Simionovici A S, Drakopoulos M, Snigirev A and Snigireva I 2001 *Nucl. Instrum. Methods A* **467–468** 944–50
- [19] Alianelli L, Sawhney K J S, Snigireva I and Snigirev A 2010 *AIP Conf. Proc.* **1234** 633–6
- [20] Ribbing C, Cederström B and Lundqvist M 2003 *Diam. Relat. Mater.* **12** 1793–9
- [21] Björkman H, Rangsten P and Hjort K 1999 *Sensors Actuators A* **78** 41–47
- [22] Ayón A A, Bayt R L and Breuer K S 2001 *Smart Mater. Struct.* **10** 1135–44
- [23] Alianelli L, Sawhney K J S, Malik A, Fox O J L, May P W, Stevens R, Loader I M and Wilson M C 2010 *J. Appl. Phys.* **108** 123107
- [24] Laermer F and Schilp A 1996 *US Patent No.* 5501893
- [25] Chen K S, Ayon A A, Xin Z and Spearing S M 2002 *J. Microelectromech. Syst.* **11** 264–75
- [26] Sawhney K J S, Dolbnya I P, Tiwari M K, Alianelli L, Scott S M, Preece G M, Pedersen U K and Walton R D 2010 *AIP Conf. Proc.* **1234** 387–90
- [27] May P W and Mankelevich Y A 2008 *J. Phys. Chem. C* **112** 12432–41
- [28] Fox O J L, Holloway J O P, Fuge G M, May P W and Ashfold M N R 2010 *MRS Proc.* **1203** J17
- [29] Hynes A M, Ashraf H, Bhardwaj J K, Hopkins J, Johnston I and Shepherd J N 1999 *Sensors Actuators A* **74** 13–17
- [30] Lai S, Johnson D J, Westerman R J, Nolan J J, Purser D and Devre M 2003 *Proc. SPIE* **4979** 43–50
- [31] Snigirev A, Snigireva I, Grigoriev M, Yunkin V, Michiel M D, Vaughan G, Kohn V and Kuznetsov S 2009 *J. Phys.: Conf. Ser.* **186** 012072